

BIROn - Birkbeck Institutional Research Online

Zhou, Y. and Pogge von Strandmann, Philip A.E. and Zhu, M. and Ling, H. and Manning, C. and Li, D. and He, T. and Shields, G. (2020) Reconstructing Tonian seawater $87\text{Sr}/86\text{Sr}$ using calcite microspar. *Geology*, ISSN 0091-7613.

Downloaded from: <https://eprints.bbk.ac.uk/id/eprint/31131/>

Usage Guidelines:

Please refer to usage guidelines at <https://eprints.bbk.ac.uk/policies.html>
contact lib-eprints@bbk.ac.uk.

or alternatively

Reconstructing Tonian seawater $^{87}\text{Sr}/^{86}\text{Sr}$ using calcite microspar

Ying Zhou¹, Philip A.E. Pogge von Strandmann¹, Maoyan Zhu^{2,3}, Hongfei Ling⁴, Christina Manning⁵, Da Li⁴, Tianchen He⁶ and Graham A. Shields¹

¹ London Geochemistry and Isotope Centre, Institute of Earth and Planetary Sciences, University College London and Birkbeck, University of London, Gower Street, London, WC1E 6BT, UK

² State Key Laboratory of Palaeobiology and Stratigraphy and Center for Excellence in Life and Palaeoenvironment, Nanjing Institute of Geology and Palaeontology, Chinese Academy of Sciences, Nanjing 210008, China

³ College of Earth and Planetary Sciences, University of Chinese Academy of Sciences, Beijing 100049, China

⁴ School of Earth Sciences, Nanjing University, Nanjing, 210023

⁵ Department of Earth Sciences, Royal Holloway, University of London, Egham, TW20 0EX

⁶ School of Earth and Environment, University of Leeds, Leeds, LS2 9JT

ABSTRACT

The Tonian Period follows a long interval of relative stasis and leads into the climatic extremes and biological radiations of multicellular life during the Cryogenian and Ediacaran periods, respectively. However, despite its pivotal situation, it remains relatively understudied, in large part due to the lack of robust age constraints. A combination of fossil evidence, radiometric ages and isotopic constraints reveal that carbonate strata on the North China craton (NCC) were deposited between c.980 and c.920 Ma, thereby filling a gap in marine archives. Here we present $^{87}\text{Sr}/^{86}\text{Sr}$ data from selected calcite microspar cements (CMC), which filled early diagenetic ‘molar tooth’ cracks, along with data from demonstrably well-preserved bulk carbonate samples. These

new data show that seawater $^{87}\text{Sr}/^{86}\text{Sr}$ rose in stages from ~ 0.7052 at c.980 Ma to ~ 0.7063 by c.920 Ma, after which a return to low values coincided with the eruption of the Dashigou large igneous province (LIP) across the NCC. We also present a new Neoproterozoic seawater $^{87}\text{Sr}/^{86}\text{Sr}$ curve, which reveals that the general trend towards higher $^{87}\text{Sr}/^{86}\text{Sr}$ during the Tonian Period was checked repeatedly by the input of less radiogenic strontium from a series of eruptive events, both coincident with and prior to the main breakup of Rodinia. The weathering of Tonian volcanic provinces has been linked to higher carbon burial, glaciation and oxygenation due to the high phosphorus content of flood basalts. Here we show that the weathering of major volcanic provinces affected material fluxes and ocean chemistry much earlier than previously envisaged.

INTRODUCTION

The strontium isotopic composition of seawater is homogeneous around the globe within analytical precision (McArthur, 1994; Kuznetsov et al., 2012) and varies over time in response to the balance between two distinct sources of strontium: 1) less radiogenic Sr that enters the oceans via Sr exchange between seawater and ocean lithosphere and 2) isotopically variable but generally more radiogenic riverine Sr derived from the weathering of differentiated continental crust (Brass, 1976; Gaillardet et al., 2014; McArthur et al., 2012). The isotopic composition of rivers can vary considerably depending on the relative contribution from older, more radiogenic terrains versus less radiogenic mantle-derived igneous rocks, such as basalt. Strontium isotope stratigraphy (SIS) can therefore help to constrain not only the ages of sedimentary successions but also the relative influence of tectonic factors, such as sea-floor spreading, emplacement of juvenile volcanic provinces and continental weathering rates, on ocean composition (Veizer, 1989; McArthur, 1994). Although SIS is well established in Phanerozoic studies because of the abundance of

mineralogically stable biogenic materials such as low-Mg calcite shells, its application to Proterozoic strata is still dependent upon variably preserved bulk carbonate rock.

Despite inherent challenges, significant progress has been made towards constructing a Neoproterozoic seawater $^{87}\text{Sr}/^{86}\text{Sr}$ curve using bulk carbonate samples (Derry et al., 1992; Shields, 1999; Halverson et al., 2007; Kuznetsov et al., 2017), and recently Cox et al. (2016) extended their compilation to 1050 Ma (see SI for more details). All previous studies document a general increase in seawater $^{87}\text{Sr}/^{86}\text{Sr}$, from about 0.705 to 0.709, over the course of the Neoproterozoic. However, details remain speculative because most published data suffer from poor age control, such as Tonian data from Siberia and the Urals (e.g. Kuznetsov et al., 2006, 2017), and/or are difficult to correlate globally (cf. Cox et al., 2016) due to lack of biostratigraphic control and the non-uniqueness of carbon isotope trends (Melezhik et al., 2015). Nevertheless, previous studies suggest that SIS has potential for both stratigraphic correlation and environmental interpretation of Neoproterozoic events, provided that well-preserved marine carbonate samples can be placed within the improving, global stratigraphic framework.

This study improves Neoproterozoic SIS by specifically targeting demonstrably well-preserved and age-constrained examples of calcite microspar cements (CMC), which fill early diagenetic cracks, commonly referred to as ‘molar tooth structure’, and other cavities. Our new data for the North China craton fill a gap in the record between c.980 to c.920 Ma towards a new Sr isotope curve for Neoproterozoic seawater.

GEOLOGICAL BACKGROUND AND AGE MODEL

The North China Craton (NCC) has an Archean to Paleoproterozoic basement and unmetamorphosed Mesoproterozoic to Neoproterozoic sedimentary cover that was deposited in a

shallow marine environment. The Huaibei region, the research area of the present study, is situated on the southern margin of this eastern NCC block (Fig. 1) and contains a thick succession of largely carbonate strata that correlate with the Jinxian Group in the Dalian area.

Detrital zircon and intrusive diabase zircon and baddeleyite U-Pb ages indicate an early Neoproterozoic age for the Huaibei and Jinxian successions (Liu et al., 2006; Gao et al., 2009; Yang et al., 2012; Wang et al., 2012). A Tonian age is also supported by age suggestive macrofossils (Dong et al., 2008; Xiao et al., 2014), age diagnostic acritarchs (Tang et al., 2013, 2015) and limited published C-isotope (Zang and Walter, 1992; Yang et al., 2001; Zheng et al., 2004; Xiao et al., 2014) and Sr-isotope (Fairchild et al., 2000; Yang et al., 2001; Xiao et al., 2014; Kuang et al., 2011) data. Dike swarms and sills, intruded along the southeastern margin of the NCC between about 920 and 900 Ma, provide a minimum age for the successions and are named the Dashigou-CDS large igneous province or LIP (Peng et al., 2011). The similarity in intrusion ages across the NCC (including the Korean peninsula) implies that widespread crustal extension and related magmatism occurred shortly after deposition had ceased at Jinxian and Huaibei, possibly due to pre-magmatic regional uplift after ~0.92 Ga (Zhang et al., 2016; Zhu et al., 2019). Recent detrital zircon (He et al., 2016; Wan et al., 2019) and magmatic baddeleyite ages for Jinxian (Fu et al., 2015; Wang et al., 2012) and Huaibei successions (Zhu et al., 2019) constrain the maximum depositional age of uppermost carbonate successions to ~920 Ma (see SI). Based on all available geochronological data, deposition of these carbonate strata ranged between ~980 Ma and ~920 Ma (see SI).

METHODS

235 carbonate samples were collected from the Huaibei Group. In order to evaluate their suitability for Sr isotope stratigraphy, all samples underwent thorough diagenetic screening using

a combination of field-based and laboratory-based observations. Samples were initially vetted in the field whereby limestone examples of early lithified cavity-filling CMC were favoured. Samples were studied petrographically before targeted analysis of micro-drilled powder for their trace elemental as well as stable C, O and radiogenic Sr isotopic compositions.

Stable isotopes ($\delta^{13}\text{C}$ and $\delta^{18}\text{O}$) were analysed at two laboratories: the Bloomsbury Environmental Isotope Facility (BEIF) at University College London on a ThermoFinnigan Delta PLUS XP mass spectrometer attached to a ThermoScientific Gas Bench II device, and at the State Key Isotope Laboratory for Palaeobiology and Stratigraphy, Nanjing Institute of Geology and Palaeontology, Chinese Academy of Sciences (NIGPAS) on a Finnigan MAT-253 mass spectrometer fitted with a Kiel IV carbonate device. Both laboratories have controlled temperatures of $22^\circ\text{C} \pm 1^\circ\text{C}$ and humidity of $50\% \text{ RH} \pm 5\%$.

The use of trace element ratios for diagenetic screening has been discussed in many publications (McArthur, 1994; Kaufman and Knoll, 1995; Montañez et al., 1996; Jacobsen and Kaufman, 1999; Brand, 2004; Brand et al., 2012), although there are no agreed criteria (see Fig. S3). For this study, no cut off criteria have been applied, but three simple principles were applied for elemental screening: (1) low Mn/Sr mass ratio (in most cases ≤ 0.5); (2) high Sr concentration (in most cases $\geq 200 \mu\text{g/g}$); (3) Low Mg/Ca mass ratio (in most cases < 0.01). Elemental analyses were carried out at University College London, using both ICP-OES (Varian 720-ES) and quadrupole ICP-MS (Varian 820-MS). For strontium isotope analyses, a sequential leaching technique based on Bailey et al. (2000) was applied before extraction of Sr using cation exchange columns. Analyses were carried out at Royal Holloway University of London and also at Nanjing University by the lead author. Samples were leached sequentially twice in dilute acetic acid (0.13M in RHUL; 0.05M in Nanjing). Standard ion chromatography was used on the second leach (20-

70% of the total carbonate sample) to concentrate Sr and eliminate Rb before analysis by Thermal Ionisation Mass Spectrometry (TIMS: Phoenix Isotopx in RHUL with mean SRM 987 0.710240 ± 8 , 2sd and Thermo Scientific Triton in Nanjing with mean SRM 987 0.710244 ± 3 , 2sd).

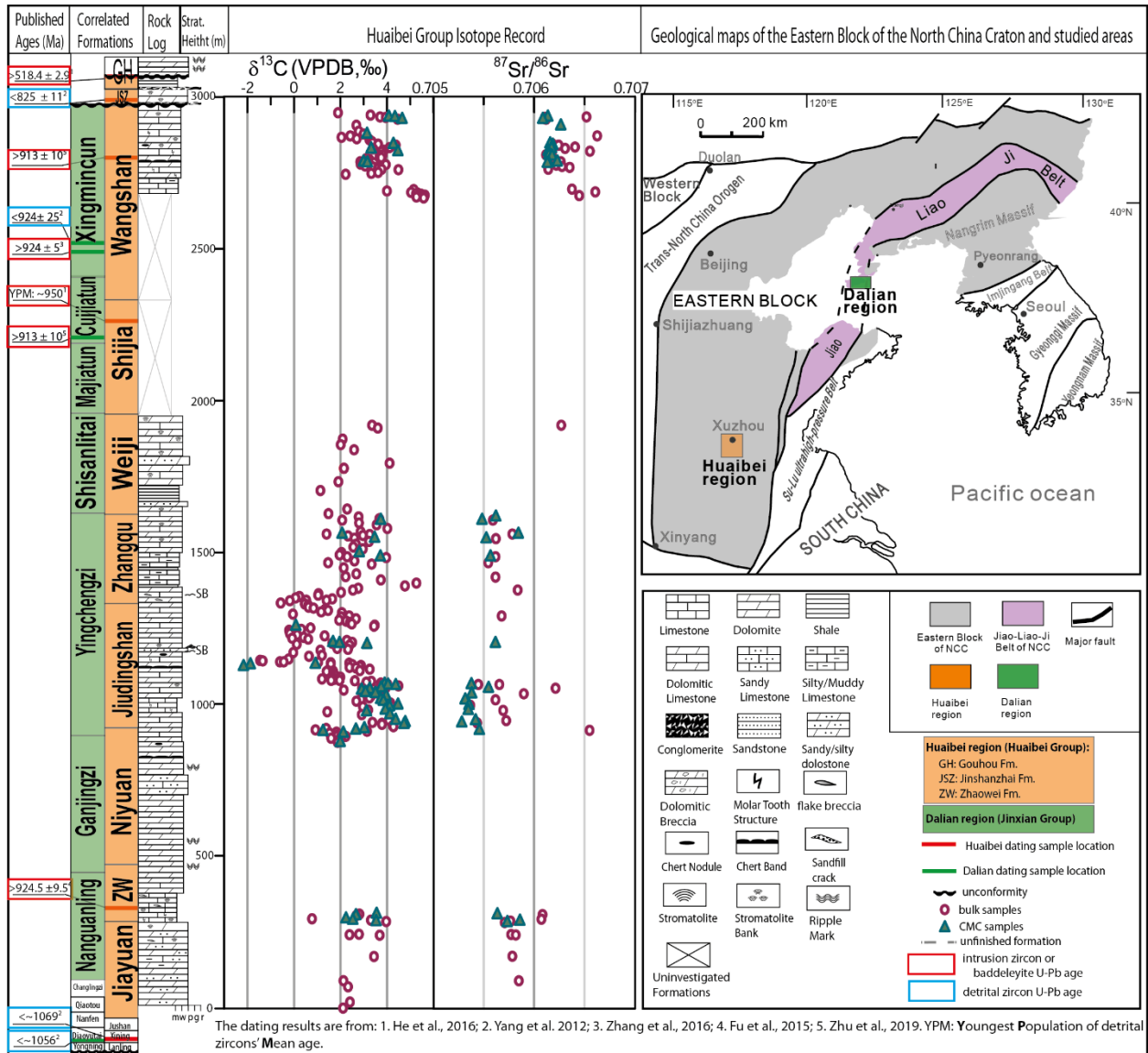


Figure 1. Carbonate carbon and strontium isotope data for the Huaibei Group in Huaibei Area. Data are shown alongside the stratigraphic log of Huaibei group, published ages for the eastern block of the NCC and inferred correlation between Huaibei and Jinxian groups. Geological map of the eastern block of NCC. Data points that did not pass the screening are not shown.

RESULTS

$\delta^{13}\text{C}_{\text{carb}}$ and $^{87}\text{Sr}/^{86}\text{Sr}$ values of Huaibei Group samples in this study are presented in Fig. 1. The data show that most Huaibei $\delta^{13}\text{C}_{\text{carb}}$ values lie between $\sim 0\text{‰}$ and $+5\text{‰}$, averaging $+2.6\text{‰}$ ($\pm 1.4\text{‰}$), which is similar to previously published early Tonian data from the southern Urals (Kuznetsov et al., 2006; 2017). Lowermost bulk and CMC $^{87}\text{Sr}/^{86}\text{Sr}$ values from best preserved samples based on the screening described above, define a gentle fall from ~ 0.7058 to ~ 0.7052 from the Jiayuan to the Jiudingshan Formation, followed by a return to ~ 0.7056 , a slight dip to ~ 0.7055 and a final rise to ~ 0.7061 through the Wangshan Fm (Fig. 1). The profile described here traces the lowest value for stratigraphic levels for which systematically less radiogenic CMC and some well preserved bulk samples are both present and to which the strictest screening has been applied. The curve, therefore, represents a conservative estimate for primary oscillations of the contemporaneous seawater $^{87}\text{Sr}/^{86}\text{Sr}$ curve. Published data from the Jinxian Group (Dalian) imply a further rise to ~ 0.7064 in the uppermost units there (Fairchild et al., 2000; Kuang et al., 2011), which are dated to c. 920 Ma (Yang et al., 2012; Zhang et al., 2016).

THE NEOPROTEROZOIC STRONTIUM ISOTOPE CURVE AND DISCUSSION

Here we use the compilation in Cox et al. (2016) as a foundation for a new seawater $^{87}\text{Sr}/^{86}\text{Sr}$ curve. The general age models of individual successions were constructed either from basic thermal subsidence modeling where possible, or by linear interpolation between correlated ages based on the assumption of constant sedimentary rates (Cox et al., 2016). The latter is used for the Huaibei data from this study and Xiao et al. (2014) in Fig 2. The trend outlined in our study is similar to that reported for the Urals by Kuznetsov et al (2017), which could indicate that the

NCC and Urals successions are of comparable age. This would be in agreement with the approximate ages assigned by Cox et al. (2016) to those successions. Furthermore, it suggests that the overall rise is followed by a return to less radiogenic values of ~ 0.7053 , documented from the Uk Formation (Kuznetsov et al., 2006).

The new curve (Fig.2 B) confirms an overall trend towards increasing seawater $^{87}\text{Sr}/^{86}\text{Sr}$ values through the whole Neoproterozoic, punctuated by nick points or falls in the curve. The general trend indicates therefore increasing influence from weathering of radiogenic continental crust relative to hydrothermal input, punctuated by intervals of lower $^{87}\text{Sr}/^{86}\text{Sr}$ when Sr sources to the oceans became less radiogenic. The part of the curve that covers the interval of this study (~ 980 – 920 Ma), shows a dip from ~ 0.7058 to ~ 0.7052 (similar to that seen also in the southern Urals), an abrupt rise to ~ 0.7064 , before a sharp fall to ~ 0.7052 by ~ 920 Ma, which approximately coincides with the eruption of the Dashigou LIP (Peng et al., 2011) that presumably increased the influx of less radiogenic Sr via both hydrothermal input and basalt weathering. This extensional magmatism could represent early signs of Rodinia break up but proximity to contemporaneous arc magmatism to the East (Kee et al., 2019) implies lithospheric thinning in a craton interior, and possibly a back-arc setting instead. Other falls in Tonian seawater $^{87}\text{Sr}/^{86}\text{Sr}$ were also preceded by LIP eruptions, e.g. the Baish, Guibei, Kangding, Shaba and later Franklin events (Fig S3) just before the onset of Sturtian ‘Snowball Earth’.

Although the weathering of LIP basalt may lead initially to a decrease in the seawater $^{87}\text{Sr}/^{86}\text{Sr}$ value (flood basalt generally exhibits near-mantle Sr isotope composition), the age distribution of widespread extension, represented by passive margins and the break-up of supercontinents, correlates well with increasing seawater $^{87}\text{Sr}/^{86}\text{Sr}$. In this regard, the staged breakup of the supercontinent that followed later Tonian LIP eruption events could have exposed

old, more radiogenic craton interiors to weathering at newly formed passive margins, and could have changed the climates of continental interiors, potentially enhancing erosion and therefore chemical weathering. Following the final phases of Rodinian assembly, this could explain why, following episodic steep dips of the global curve, seawater $^{87}\text{Sr}/^{86}\text{Sr}$ continued to rise toward its eventual high point of ~ 0.709 (Godderis et al., 2017).

Our new updated compilation of strontium isotopes (Fig. 2: B) and large igneous provinces (detail in Fig. S3) hints that the weathering of large igneous provinces had a considerable influence on ocean composition well before the postulated timing of Rodinia break up. Chemical weathering of freshly erupted mafic volcanic rock at low latitudes was likely a major source of nutrient phosphorus to the Tonian ocean (Horton, 2015; Gernon et al., 2016; Cox et al., 2016; Jenkyns, 2010; Pogge Von Strandmann et al., 2013), rendered oligotrophic and ferruginous after prolonged denudation of the long-lived supercontinent Rodinia (Guilbaud et al., 2015). Nutrient input into a largely anoxic ocean would have driven carbon (and potentially also pyrite) burial at productive ocean margins, while the subsequent oxygenation could conceivably have facilitated the opportunistic radiation of large, aerobic eukaryotes reported from the NCC (Dong et al., 2008; Tang et al., 2013, 2015). Pending further study, and consistent with reports of major C-isotope fluctuations in these and correlative successions (Hua and Cao, 2004; Xiao et al., 2014; Park et al., 2016; this paper), we postulate an earlier, more eventful end to the ‘boring billion’ than previously envisaged.

CONCLUSIONS

This is the first study that specifically uses carbonate components, in this case demonstrably early and isotopically pristine, cavity-filling calcite microspar cements (CMC) as

well as well preserved bulk carbonate, to reconstruct Neoproterozoic seawater $^{87}\text{Sr}/^{86}\text{Sr}$. Together with published data, we document a series of oscillations in $^{87}\text{Sr}/^{86}\text{Sr}$ that can plausibly be linked to the weathering of known volcanic provinces (Fig. 2). Although the weathering of large igneous provinces has previously been implicated in end-Tonian events coincident with supercontinent break up, we conclude that the weathering of flood basalts exerted a considerable influence on ocean composition well before the postulated break up of Rodinia.

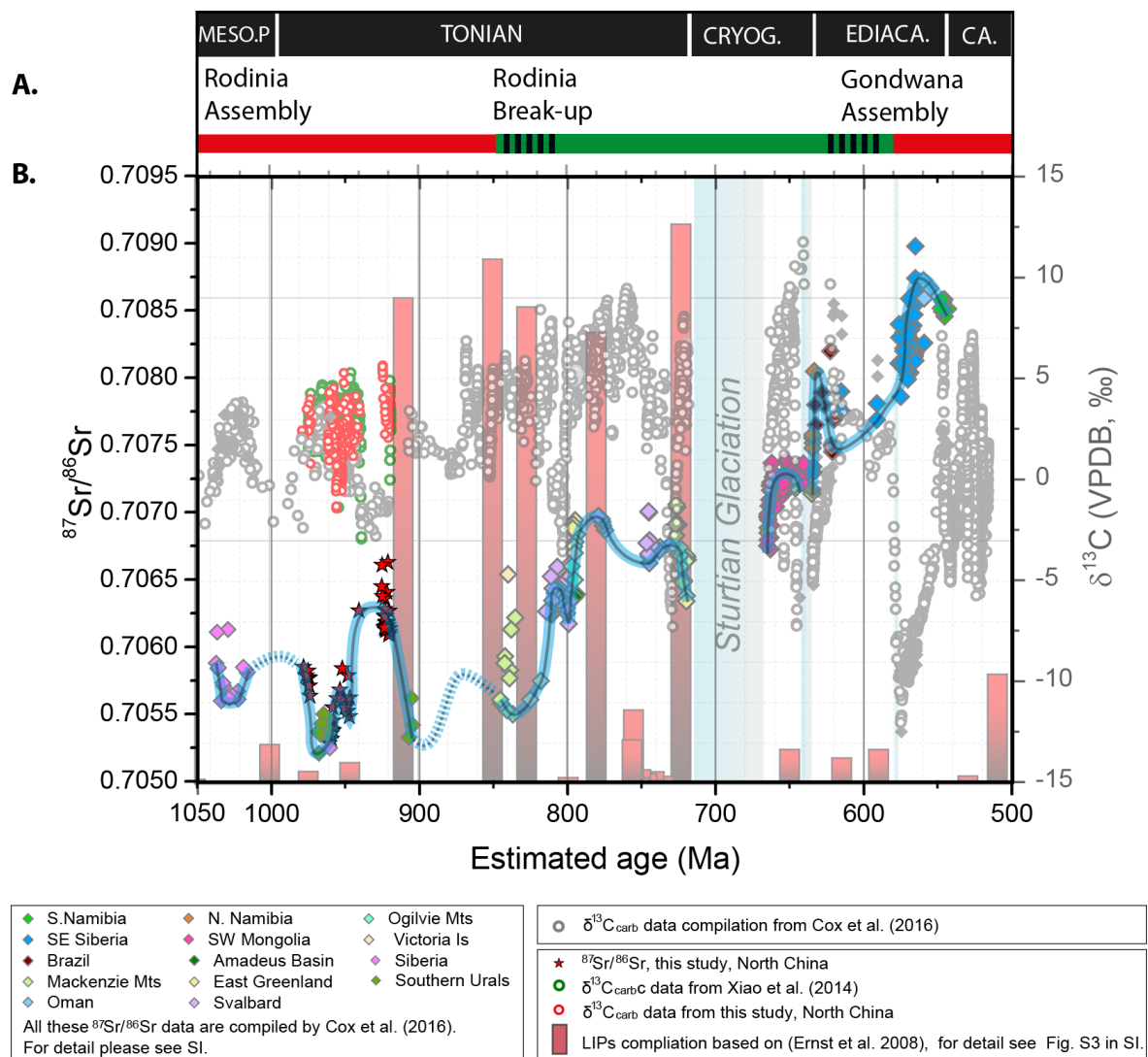


Figure 2. Isotopic evolution of Neoproterozoic seawater: Proposed Neoproterozoic seawater $^{87}\text{Sr}/^{86}\text{Sr}$ curve (black line with blue halo); a new compilation of global carbonate $\delta^{13}\text{C}$ (grey circles); an updated LIPs record during 1050 – 500 Ma (the bar heights indicate the size of the LIP); and the supercontinent cycle during 1050 – 500 Ma (Bradley, 2008). The light blue columns in the background mark three known glaciations; from old to young: Sturtian, Marinoan and Gaskiers. The updated compilation of Large Igneous Provinces from 1050 – 500 Ma is based on (Ernst et al., 2008) and an updated compilation at <http://www.largeigneousprovinces.org/>. Additionally, the sizes of the ~920 Ma Dashigou LIP and the Bahia – Ganila LIP were taken from Peng et al. (2011) and Chaves et al. (2018) (for more detail see Fig. S3.). For the $\delta^{13}\text{C}$ data, the grey circles are published data, compiled by Cox et al. (2016); green circles are data from Xiao et al. (2014); red circles are from this study. For the $^{87}\text{Sr}/^{86}\text{Sr}$ data, the red stars are data from this study; details of all other data can be found in Cox et al. (2016).

ACKNOWLEDGMENTS

This study has been supported by the NERC - NSFC co-funded research programme: Co-Evolution of Life and the Planet and project ‘Re-inventing the planet: the Neoproterozoic revolution in oxygenation, biogeochemistry and biological complexity’ (NE/1005978/1 to GS & NSFC 41661134048 to MZ), and Strategic Priority Research Program (B) of the Chinese Academy of Sciences (CAS) (XDB18000000) to MZ. The lead author acknowledges Xiaoming Chen, Jing Liu (Stable Isotope lab, Nanjing Institute of Geology and Palaeontology), Gary Tarbuck and Anne-Lise Jourdan (UCL) for their technical support, and Zhengxiao Guo (UCL) for his supervisory role.

REFERENCES CITED

- Bailey, T.R., McArthur, J.M., Prince, H., and Thirlwall, M.F., 2000, Dissolution methods for strontium isotope stratigraphy: Whole rock analysis: *Chemical Geology*, v. 167, p. 313–319, doi: 10.1016/S0009-2541(99)00235-1.
- Bradley, D.C., 2008, Passive margins through earth history: *Earth-Science Reviews*, v. 91, p. 1–26, doi: 10.1016/j.earscirev.2008.08.001.
- Brand, U., 2004, Carbon, oxygen and strontium isotopes in Paleozoic carbonate components: An evaluation of original seawater-chemistry proxies: *Chemical Geology*, v. 204, p. 23–44, doi: 10.1016/j.chemgeo.2003.10.013.
- Brand, U., Jiang, G., Azmy, K., Bishop, J., and Montañez, I.P., 2012, Diagenetic evaluation of a Pennsylvanian carbonate succession (Bird Spring Formation, Arrow Canyon, Nevada, U.S.A.) - 1: Brachiopod and whole rock comparison: *Chemical Geology*, v. 308–309, p. 26–39, doi: 10.1016/j.chemgeo.2012.03.017.
- Brass, G.W., 1976, The variation of the marine $^{87}\text{Sr}/^{86}\text{Sr}$ ratio during Phanerozoic time: interpretation using a flux model: *Geochimica et Cosmochimica Acta*, v. 40, p. 721–730, <http://link.springer.com/10.1134/S0869593812060044>.
- Chaves, A.D.O., Ernst, R.E., Söderlund, U., Wang, X., and Naeraa, T., 2018, The 920 – 900 Ma Bahia-Gangila LIP of the São Francisco and Congo cratons and link with Dashigou-Chulan LIP of North China craton : New insights from U-Pb geochronology and geochemistry: *Precambrian Research*, p. 0–1, doi: 10.1016/j.precamres.2018.08.023.
- Cox, G.M., Halverson, G.P., Stevenson, R.K., Vokaty, M., Poirier, A., Kunzmann, M., Li, Z.-X., Denyszyn, S.W., Strauss, J. V., and Macdonald, F.A., 2016, Continental flood basalt weathering as a trigger for Neoproterozoic Snowball Earth: *Earth and Planetary Science*

Letters, v. 446, p. 89–99, doi: 10.1016/j.epsl.2016.04.016.

Derry, L.A., Kaufman, A.J., and Jacobsen, S.B., 1992, Sedimentary cycling and environmental change in the late Proterozoic: evidence from stable isotopes: *Geochimica et Cosmochimica Acta*, v. 56, p. 1317–1329.

Dong, L., Xiao, S., Shen, B., Yuan, X., Yan, X., and Peng, Y., 2008, Restudy of the worm-like carbonaceous compression fossils *Protoarenicola*, *Pararenicola*, and *Sinosabellidites* from early Neoproterozoic successions in North China: *Palaeogeography, Palaeoclimatology, Palaeoecology*, v. 258, p. 138–161, doi: 10.1016/j.palaeo.2007.05.019.

Ernst, R.E., Wingate, M.T.D., Buchan, K.L., and Li, Z.X., 2008, Global record of 1600–700 Ma Large Igneous Provinces (LIPs): Implications for the reconstruction of the proposed Nuna (Columbia) and Rodinia supercontinents: *Precambrian Research*, v. 160, p. 159–178, doi: 10.1016/j.precamres.2007.04.019.

Fairchild, I.J., Herrington, P.M., and Song, T., 2000, Controls on Sr and C isotope compositions of Neoproterozoic Sr-rich limestones of East Greenland and North China: *Special Publications of SEPM*, v. 67, p. 297–313.

Fu, X., Zhang, S., Li, H., Ding, J., Li, H., Yang, T., Wu, H., Yuan, H., and Lv, J., 2015, New paleomagnetic results from the Huaibei Group and Neoproterozoic mafic sills in the North China Craton and their paleogeographic implications: *Precambrian Research*, v. 269, p. 90–106, doi: 10.1016/j.precamres.2015.08.013.

Gaillardet, J., Viers, J., and Dupre, B., 2014, Trace Elements in River Waters:., doi: 10.1016/B978-0-08-095975-7.00507-6.

Gao, L., Zhang, C., Liu, P., Tang, F., Song, B., and Ding, X., 2009, Reclassification of the Meso- and Neoproterozoic chronostratigraphy of North China by SHRIMP zircon ages: *Acta*

Geologica Sinica - English Edition, v. 83, p. 1074–1084.

Gernon, T.M., Hincks, T.K., Tyrrell, T., Rohling, E.J., and Palmer, M.R., 2016, Snowball Earth ocean chemistry driven by extensive ridge volcanism during Rodinia breakup: *Nature Geoscience*, v. 9, p. 242–248, doi: 10.1038/ngeo2632.

Godderis, Y., Le Hir, G., Macouin, M., Donnadiou, Y., Hubert-Theou, L., Dera, G., Aretz, M., Fluteau, F., Li, Z.X., and Halverson, G.P., 2017, Paleogeographic forcing of the strontium isotopic cycle in the Neoproterozoic: *Gondwana Research*, v. 42, p. 151–162, doi: 10.1016/j.gr.2016.09.013.

Guilbaud, R., Poulton, S.W., Butterfield, N.J., Zhu, M., and Shields-zhou, G. a, 2015, A global transition to ferruginous conditions in the early Neoproterozoic oceans: *Nature Geoscience*, v. 8, p. 466–470, doi: 10.1038/NGEO2434.

Halverson, G.P., Dudás, F.Ö., Maloof, A.C., and Bowring, S.A., 2007, Evolution of the $^{87}\text{Sr}/^{86}\text{Sr}$ composition of Neoproterozoic seawater: *Palaeogeography, Palaeoclimatology, Palaeoecology*, v. 256, p. 103–129, doi: 10.1016/j.palaeo.2007.02.028.

Horton, F., 2015, Did phosphorus derived from the weathering of large igneous provinces fertilize the Neoproterozoic ocean? *Geochemistry Geophysics Geosystems*, v. 16, p. 1723–1738, doi: 10.1002/2015GC005792. Received.

Hua, H., and Cao, R., 2004, An abrupt variation event of stromatolitic microstructures in the Neoproterozoic and its origination background: *Acta Palaeontologica Sinica*, v. 43, p. 234–245.

Jacobsen, S.B., and Kaufman, A.J., 1999, The Sr, C and O isotopic evolution of neoproterozoic seawater-comment: *Chemical Geology*, v. 161, p. 37–57, doi: 10.1016/S0009-2541(01)00268-6.

- Jenkyns, H.C., 2010, Geochemistry of oceanic anoxic events: *Geochemistry, Geophysics, Geosystems*, v. 11, p. 1–30, doi: 10.1029/2009GC002788.
- Kaufman, A.J., and Knoll, A.H., 1995, Neoproterozoic variations in the C-isotopic composition of seawater: stratigraphic and biogeochemical implications: *Precambrian Research*, v. 73, p. 27–49, doi: 10.1016/0301-9268(94)00070-8.
- Kee, W.S., Kim, S.W., Kwon, S., Santosh, M., Ko, K., and Jeong, Y.J., 2019, Early Neoproterozoic (ca. 913–895 Ma) arc magmatism along the central–western Korean Peninsula: Implications for the amalgamation of Rodinia supercontinent: *Precambrian Research*, v. 335, p. 105498, doi: 10.1016/j.precamres.2019.105498.
- Kuang, H., Yongqing, L., Peng, N., and Liu, L., 2011, Geochemistry of the Neoproterozoic molartooth carbonates in Dalian, eastern Liaoning, China, and its geological implications: *Earth Science Frontiers*, v. 18, p. 25–40.
- Kuznetsov, A.B., Bekker, A., Ovchinnikova, G. V., Gorokhov, I.M., and Vasilyeva, I.M., 2017, Unradiogenic strontium and moderate-amplitude carbon isotope variations in early Tonian seawater after the assembly of Rodinia and before the Bitter Springs Excursion: *Precambrian Research*, v. 298, p. 157–173, doi: 10.1016/j.precamres.2017.06.011.
- Kuznetsov, a. B., Semikhatov, M. a., and Gorokhov, I.M., 2012, The Sr isotope composition of the world ocean, marginal and inland seas: Implications for the Sr isotope stratigraphy: *Stratigraphy and Geological Correlation*, v. 20, p. 501–515, doi: 10.1134/S0869593812060044.
- Kuznetsov, a. B., Semikhatov, M. a., Maslov, a. V., Gorokhov, I.M., Prasolov, E.M., Krupenin, M.T., and Kislova, I. V., 2006, New data on Sr-and C-isotopic chemostratigraphy of the Upper Riphean type section (Southern Urals): *Stratigraphy and Geological Correlation*, v.

14, p. 602–628, doi: 10.1134/S0869593806060025.

Liu, Y., Gao, L., Liu, Y., Song, B., and Wang, Z., 2006, Zircon U-Pb dating for the earliest Neoproterozoic mafic magmatism in the southern margin of the North China Block: Chinese Science Bulletin, v. 51, p. 2375–2382, doi: 10.1007/s11434-006-2114-0.

McArthur, J.M., 1994, Recent trends in strontium isotope stratigraphy: Terra Nova, v. 6, p. 331–358, doi: 10.1111/j.1365-3121.1994.tb00507.x.

McArthur, J.M., Howarth, R.J., and Shields, G.A., 2012, Strontium Isotope Stratigraphy: The Geologic Time Scale, p. 127–144, doi: 10.1016/B978-0-444-59425-9.00007-X.

Melezhik, V.A., Ihlen, P.M., Kuznetsov, A.B., Gjelle, S., Solli, A., Gorokhov, I.M., Fallick, A.E., Sandstad, J.S., and Bjerkgård, T., 2015, Pre-Sturtian (800-730Ma) depositional age of carbonates in sedimentary sequences hosting stratiform iron ores in the Uppermost Allochthon of the Norwegian Caledonides: A chemostratigraphic approach: Precambrian Research, v. 261, p. 272–299, doi: 10.1016/j.precamres.2015.02.015.

Montanez, I.P., Banner, J.L., Osleger, D.A., Borg, L.E., and Bosserman, P.J., 1996, Integrated Sr isotope variations and sea-level history of middle to Upper Cambrian platform carbonates: Implications for the evolution of Cambrian seawater $^{87}\text{Sr}/^{86}\text{Sr}$: Geology, v. 24, p. 917–920, doi: 10.1130/0091-7613(1996)024<0917:ISIVAS>2.3.CO.

Park, H., Zhai, M., Yang, J., Peng, P., Kim, J., Zhang, Y., Kim, M., Park, U., and Feng, L., 2016, Deposition age of the Sangwon Supergroup in the Pyongnam basin (Korea) and the Early Tonian negative carbon isotope interval: Acta Petrologica Sinica, v. 32, p. 2181–2195.

Peng, P., Bleeker, W., Ernst, R.E., Söderlund, U., and McNicoll, V., 2011, U–Pb baddeleyite ages, distribution and geochemistry of 925Ma mafic dykes and 900Ma sills in the North China craton: Evidence for a Neoproterozoic mantle plume: Lithos, v. 127, p. 210–221, doi:

10.1016/j.lithos.2011.08.018.

Pogge Von Strandmann, P.A.E., Jenkyns, H.C., and Woodfine, R.G., 2013, Lithium isotope evidence for enhanced weathering during Oceanic Anoxic Event 2: *Nature Geoscience*, v. 6, p. 668–672, doi: 10.1038/ngeo1875.

Shields, G.A., 1999, Working towards a new stratigraphic calibration scheme for the Neoproterozoic-Cambrian: *ECLOGAE GEOLOGICAE HELVETIAE*, v. 92, p. 221–233.

Tang, Q., Pang, K., Xiao, S., Yuan, X., Ou, Z., and Wan, B., 2013, Organic-walled microfossils from the early Neoproterozoic Liulaobei Formation in the Huainan region of North China and their biostratigraphic significance: *Precambrian Research*, v. 236, p. 157–181, doi: 10.1016/j.precamres.2013.07.019.

Tang, Q., Pang, K., Yuan, X., Wan, B., and Xiao, S., 2015, Organic-walled microfossils from the Tonian Gouhou Formation, Huaibei region, North China Craton, and their biostratigraphic implications: *Precambrian Research*, v. 266, p. 296–318, doi: <http://dx.doi.org/10.1016/j.precamres.2015.05.025>.

Veizer, J., 1989, Strontium Isotopes in Seawater through Time: *Annual Review of Earth and Planetary Sciences*, v. 17, p. 141–167.

Wang, Q., Yang, D., and Xu, W., 2012, Neoproterozoic basic magmatism in the southeast margin of North China Craton: Evidence from whole-rock geochemistry, U-Pb and Hf isotopic study of zircons from diabase swarms in the Xuzhou-Huaibei area of China: *Science China Earth Sciences*, v. 55, p. 1461–1479, doi: 10.1007/s11430-011-4237-7.

Xiao, S., Shen, B., Tang, Q., Kaufman, A.J., Yuan, X., Li, J., and Qian, M., 2014, Biostratigraphic and chemostratigraphic constraints on the age of early Neoproterozoic carbonate successions in North China: *Precambrian Research*, v. 246, p. 208–225, doi:

10.1016/j.precamres.2014.03.004.

Yang, D. Bin, Xu, W.L., Xu, Y.G., Wang, Q.H., Pei, F.P., and Wang, F., 2012, U-Pb ages and Hf isotope data from detrital zircons in the Neoproterozoic sandstones of northern Jiangsu and southern Liaoning Provinces, China: Implications for the Late Precambrian evolution of the southeastern North China Craton: *Precambrian Research*, v. 216–219, p. 162–176, doi: 10.1016/j.precamres.2012.07.002.

Yang, J., Zheng, W., Wang, Z., and Tao, X., 2001, Age determining of the upper Precambrian system of Northern Jiangsu-Anhui by using Sr and C isotopes: *Journal of Stratigraphy* (in Chinese), v. 25, p. 44–47.

Zang, W.-L., and Walter, M.R., 1992, Late Proterozoic and Early Cambrian microfossils and biostratigraphy, Northern Anhui and Jiangsu: *Precambrian Research*, v. 57, p. 243–323.

Zhang, S., Zhao, Y., Ye, H., and Hu, G.H., 2016, Early Neoproterozoic emplacement of the diabase sill swarms in the Liaodong Peninsula and pre-magmatic uplift of the southeastern North China Craton: *Precambrian Research*, v. 272, p. 203–225, doi: 10.1016/j.precamres.2015.11.005.

Zheng, W., Yang, J., Hong, T., Tao, X., and Wang, Z., 2004, Sr and C Isotopic Correlation and the Age Boundary Determination for the Neoproterozoic in the Southern Liaoning and Northern Jiangsu Northern Anhui Provinces: *Geological Journal of China Universities* (in Chinese), v. 10.

Zhu, R., Ni, P., Wang, G., Ding, J., Fan, M., and Ma, Y., 2019, Geochronology, geochemistry and petrogenesis of the Laozhaishan dolerite sills in the southeastern margin of the North China Craton and their geological implication: *Gondwana Research*, v. 67, p. 131–146, doi: 10.1016/j.gr.2018.10.016.

